

Original Research Communication

Mitochondrial Ferritin is a HIF1 α -Inducible Gene that Protects from Hypoxia-Induced Cell Death in Brain

Qiong Wu^{1, 2§}, Wen-Shuang Wu^{1§}, Lin Su¹, Xin Zheng¹, Wen-Yue Wu¹, Paolo Santambrogio²,
Yu-Jing Gou¹, Qian Hao¹, Pei-Na Wang¹, Ya-Ru Li¹, Bao-Lu Zhao¹, Guangjun Nie⁴, Sonia Levi²,
^{3*} & Yan-Zhong Chang^{1*}

¹ Laboratory of Molecular Iron Metabolism, The Key Laboratory of Animal Physiology, Biochemistry and Molecular Biology of Hebei Province, College of Life Science, Hebei Normal University, Shijiazhuang, Hebei Province, China;

² San Raffaele Scientific Institute, Division of Neuroscience, 20132 Milano, Italy;

³ University Vita-Salute San Raffaele, 20132 Milano, Italy;

⁴ CAS Key Laboratory for Biomedical Effects of Nanomaterials and Nanosafety, National Center for Nanoscience and Technology, Beijing China.

[§]These two authors contributed equally to this work.

Running title: FtMt expression is controlled by HIF-1 α

* Correspondence

Sonia Levi, PhD, Professor, Vita-Salute San Raffaele University and San Raffaele Scientific Institute, Via Olgettina 58, 20132 Milano, ITALY.

Tel: 39-02-26434755, Fax: 39-02-26434844, E-mail: levi.sonia@hsr.it

Yan-Zhong Chang, PhD, Professor, Laboratory of Molecular Iron Metabolism, College of Life Science, Hebei Normal University, 20, Nanerhuan Eastern Road, Shijiazhuang, Hebei Province, 050024, People's Republic of China.

E-mail: frankyzchang@yahoo.com.hk

Tel: 86-311-80786311, Fax: 86-311-80786311.

Key words: mitochondrial ferritin, HIF-1 α hypoxia-induced apoptosis, ROS

Word count=5906

Reference number=68

Gray scale illustration= 8

Color illustration =7 (online 7 and hardcopy 0)

Abstract

Mitochondrial Ferritin (FtMt) is preferentially expressed in cell types of high metabolic activity and oxygen consumption, which is consistent with its role of sequestering iron and preventing oxygen-derived redox damage. As of yet, the mechanisms of FtMt regulation and the protection FtMt affords remain largely unknown. Here, we report that hypoxia-inducible-factor 1 α (HIF-1 α) can upregulate FtMt expression. We verify one functional hypoxia response element (HRE) in the positive regulatory region and two HREs possessing HIF-1 α binding activity in the minimal promoter region of the human *FTMT* gene. We also demonstrate that FtMt can alleviate hypoxia-induced brain cell death by sequestering uncommitted iron, whose levels increase with hypoxia in these cells. In the absence of FtMt, this catalytic metal excess catalyzes the production of cytotoxic reactive oxygen species (ROS). Thus, the cell ability to increase expression of FtMt during hypoxia may be a skill to avoid tissue damage derived from oxygen limitation.

Introduction

Mitochondrial ferritin (FtMt) is a mitochondrial iron storage protein encoded by an intronless gene (*FTMT*) on chromosome 5q23.1. FtMt plays an important role in the distribution of iron within mitochondria (26). The protein is ubiquitously expressed in primates (human, chimpanzee and macaque)(12,26,62), in other mammals (mouse, rat and dog)(12) and in insects, such as *Drosophila melanogaster* (32). FtMt has also been identified in plants, such as cucumber (15,53,65). The full sequence and 3D structure of FtMt are remarkably similar to those of ferritin-H (Ft-H), and the residues of the ferroxidase center are all conserved (25). Overexpression of FtMt in HeLa cells showed this protein is functionally active in incorporating iron, apparently even more efficient than Ft-H and ferritin-L (Ft-L) (11). These discoveries demonstrate that FtMt is structurally and functionally similar to the cytosolic ferritins.

Numerous reports have documented FtMt's involvement in several pathological processes. FtMt accumulates in high amounts in erythroblasts of subjects with impaired heme synthesis (26) and in ring sideroblasts from sideroblastic anemia patients (9). Our recent study reveals that mitochondrial ferritin can protect the murine myocardium from acute exhaustive exercise injury (59). Moreover, FtMt had a profound protective role in neurodegenerative diseases (61). Increased FtMt levels were detected in the human substantia nigra (SN) from restless legs syndrome (RLS) patients (49), in cardiomyocytes of Friedreich Ataxia (FRDA) patients (24) and in the cerebral cortex of Alzheimer's disease (AD) patients (56). FtMt can also abrogate oxidative damage and rescue respiratory function in FRDA (6,66) or attenuate the neurotoxicity induced by 6-hydroxydopamine (6-OHDA) (45), MPTP (63) and β -Amyloid ($A\beta$) (60) both in Parkinson's disease (PD) and AD. In addition, *FTMT* mutations were identified in patients suffering movement disorders (8) and in one case, age-related macular degeneration (AMD) (50), suggesting that FtMt deficiency may decrease protection from iron-dependent oxidative stress in mitochondria. Increasing FtMt has been proposed as a therapeutic strategy to inhibit tumor growth by decreasing cytosolic iron levels (34,46). All of these findings are indicative of vital roles for FtMt in antioxidant response and iron metabolism. The presence of free redox-active iron

(Fe^{2+}) in a cell can contribute to the formation of free radicals that increase cellular oxidative stress via the Fenton reaction, which entails Fe^{2+} -catalyzed production of highly toxic hydroxyl radicals (52). FtMt can sequester “uncommitted” iron in its spherical shells in a form that is not accessible for Fenton chemistry, thus it can protect mitochondria from oxidative damage. Therefore, it is not surprising that FtMt is preferentially expressed in cells with vigorous metabolic activity and oxygen consumption, which is associated with comparatively elevated production of reactive oxygen species (ROS). This is congruent with FtMt’s role of mitigating redox damage from the combination of catalytic iron and oxygen (41,48). However, overexpression of FtMt caused cytosolic iron deprivation (11) and sensitized cells to oxidative stress (31,35,42). Increased FtMt also may lead to pathogenic cytosolic iron deprivation in RLS (49).

In contrast to the relatively abundant functional studies, little attention has been devoted to FtMt regulation. The absence of functional iron responsive element (IRE) sequences in FtMt mRNA is consistent with its iron independent expression. Recently published data sheds light on the human *FTMT* promoter study in which the analyzed putative promoter region comprises the minimal promoter as well as a positive and a negative transcriptional factors target regions and provides new evidence as to the transcriptional and epigenetic regulatory mechanisms of this gene (17). However, the detailed mechanisms governing *FTMT* regulation are yet to be clarified. The preferential expression of the gene in cells with high oxygen consumption suggests an intimate relationship between FtMt and oxygen availability.

Appropriate responses to low ambient oxygen are largely mediated through transcriptional activation of genes by hypoxia inducible factor (HIF) proteins. HIFs are heterodimers containing a HIF- α and a HIF- β subunit. The HIF- β subunit is a constitutively expressed partner for multiple basic-helix/loop/helix per-Arnt-sim (bHLH-PAS) transcription factors. The HIF- α subunit, however, is regulated in response to changes in cellular oxygen availability (54). HIF-1 α , one subunit of the HIF-1 heterodimer, has been the most extensively studied. In hypoxic environments, or hypoxia-mimicking conditions in normoxia, HIF-1 α is stabilized and translocated to the nucleus, binding, with HIF-1 β , to

hypoxia-response-elements (HREs) of genes, thus activating the hypoxia transcriptional program (13,18,21,47,55). In the present study, we found that HIF-1 α can activate the expression of FtMt *in vitro* and *in vivo*. Furthermore, depletion of HIF-1 α by RNA interference (RNAi) in cells and conditional knockout (KO) of HIF-1 α in mice, abolished the upregulation of FtMt in response to hypoxic treatment. We therefore hypothesized that mitochondrial ferritin is a gene regulated by hypoxia. To explore the regulatory mechanisms, we examined the human *FTMT* promoter region and tested six potential HREs present in the 5' untranslated region (UTR) upstream of ATG codon *in silico*. In addition, we show a stimulation of oxidative stress and cell death after hypoxia treatment. Altogether, here we show that HIF-1 α is involved in the regulation of FtMt in hypoxia and FtMt plays an important protective role in hypoxia by reducing redox damage.

Results

Mitochondrial ferritin (FtMt) levels are elevated under hypoxia *in vivo* and *in vitro*

To explore the roles that FtMt may play during hypoxia, six adult mice were kept under continuous hypobaric hypoxia (HH) for 18 h in a hypobaric chamber with a simulated altitude of 8000 m (oxygen content is around 8.5%, pO₂ is about 7.5KPa). We studied the cortex and hippocampus regions in the brains of mice due to the particular vulnerability of these regions to hypoxic stress (19,67). The level of *Ftmt* mRNA and FtMt protein in the cortices and hippocampi (Hippo) of mice treated with or without hypoxia were then measured by quantitative real time PCR (qRT-PCR) and immunoblotting, respectively (Fig 1A and 1B). Because of the high identity between FtMt and Ft-H, we validated the specificity of the FtMt antibody in immunoblots from rat testis lysate (Fig S1). In the HH group, both the *Ftmt* mRNA and FtMt protein were increased compared to control group (Fig 1A and 1B).

In vitro, we observed the same phenotype in the C6 glioma cell line when maintained in 1% O₂ for up to 12 hours or with different concentrations of CoCl₂, as CoCl₂ is often used as a hypoxia-mimetic agent to simulate hypoxia under normal oxygen conditions (1); the level of *Ftmt* mRNA, as determined by reverse transcription-PCR, was increased in the treated cells compared to the controls (Fig 1C and 1D), while the amount of FtMt protein was consistently changed along with the mRNA levels (Fig 1E and 1F).

Increased FtMt expression under hypoxia is accompanied by changes in HIF-1 α

HIF-1 α has been largely studied for its role in cell survival under conditions of oxygen deprivation (hypoxia) where it helps to restore oxygen homeostasis by inducing glycolysis, erythropoiesis and angiogenesis (20,43,58). HIF-1 α can accumulate under hypoxia or treatment with a hypoxia-mimetic agent such as CoCl₂. As expected, we found HIF-1 α protein was elevated in C6 cells after treatment with hypoxia (1% O₂) or with CoCl₂ (Fig 2A and 2B). Previous reports have demonstrated that YC-1 inhibits HIF-1 α (3,28). When C6 cells were treated with the YC-1 (30 μ M) plus 1% O₂ for 12 h, both FtMt and HIF-1 α protein levels were decreased (by nearly 45% and 65%, respectively) compared to the untreated cells (Fig 2C). Furthermore, when we depleted the HIF-1 α protein level by RNAi, we also found an approximately 40% reduction in FtMt protein amounts (Fig 2D) which were consistent with the effects of HIF-1 α inhibition with YC-1.

Conditional knockout of HIF-1 α in mouse neurons blocks hypoxia-induced elevation of FtMt in the hippocampus

HIF-1 α was specifically inactivated in neurons by crossing C57BL/6 *HIF-1 α ^{lox/lox}* mice (Control) with Thy1-Cre C57BL/6 transgenic mice (Δ *HIF-1 α*). The mice were then placed in a hypoxic chamber with 18 h continuous hypobaric hypoxia. We first checked the localization of FtMt in the hippocampi in the control groups (Control, Control + HH), using double immunostaining with antibodies specific for cellular markers in brain (green): NeuN for neurons, glial fibrillary acidic protein (GFAP) for astrocytes and Iba1 for microglia, along with FtMt (red). These experiments revealed that FtMt is expressed mainly in the hippocampal neurons, suggesting a cell-specific regulation of FtMt (Fig S2). In addition, immunostaining showed a higher FtMt expression (red) in the Control + HH group (~2.4-fold vs the Control group, Fig 2Ei) compared to the Controls under normoxia. Importantly, we found no significant differences in FtMt expression in the Δ *HIF-1 α* mice in the differing oxygen levels (Fig 2Ei-Eii). Moreover, double immunostaining with the mitochondrial marker (COX IV, green) and FtMt showed that our FtMt antibody specifically recognizes a protein in mitochondria (Fig 2Eiii).

HIF-1 α activates FtMt expression via HRE sites in the *FTMT* promoter region.

In order to investigate whether HREs may be present in the *FTMT* promoter region, we analyzed the evolutionarily conserved region upstream of the transcriptional starting site (TSS) *in silico*. In this region, the sequence similarity between human and rat or mouse was ~70%, and over 90% among the primates (Fig 3A). We found 6 potential HREs upstream of the TSS in human *FTMT* (Fig 3B). The matrix similarity from different databases is provided in Table 1. From the alignment, we can see the same location of HREs among the primates. Hence, we took the human *FTMT* promoter as a template and used a series of 3' and 5' deletions within the promoter to test the activities of each possible HRE using dual luciferase reporter (DLR) assays in HeLa cells, whose responsiveness to the hypoxia treatment was followed by HIF-1 α protein detection in immunoblot (Fig 3C and 3D). We chose this cellular system because it was easier to transfect with varied reporter plasmids than SH-SY5Y or C6 cells. In the 3' deletion assay, the -1884/-777 group, which contained only the predicted HRE1 sequence, exhibited a nearly 5-fold increase in luciferase activity after a 1% O₂ treatment, with respect to the control group (20% O₂). The -1884/-521 group, comprising predicted HRE1 and HRE2 sites, exhibited a 3.5-fold increase in hypoxia (Fig 3E). In the 5' deletion luciferase assays, the -491/+9 and -217/+9 groups, which include the predicted HRE4-HRE6 sequence, displayed the highest activities after hypoxia treatment (~5-6 fold) (Fig 3F). All the data suggest that the binding activities of HIF-1 α to the HREs are located in the putative *FTMT* promoter region from -1884 to -521 and from -491 to +9.

To further investigate the HIF-1 α binding abilities among the predicted HREs, we next performed electrophoretic mobility shift assays (EMSA) to investigate the three HREs that are located in the minimal promoter region which is from -491 to -1 of the *FTMT* promoter region (17) (HRE4, HRE5 and HRE6) and chromatin immunoprecipitation (ChIP) assays to study functional roles of HRE1, HRE2 and HRE3.

Consistent with our findings in C6 cells (Fig 1E, Fig 2A), we detected elevated levels of FtMt and HIF-1 α proteins also in the human glioma cell line, U251, when exposed to 1% O₂ for 12 h (Fig 4A and 4B). From the EMSA assays on U251 cell line, we found only the probes containing HRE5 and HRE6 showed binding activities, with higher levels of binding

in extracts from cells treated with 1% O₂, while the probe containing HRE4 gave negative results even with extracts from cells exposed to the hypoxic environment (Fig 4C).

In addition, we analyzed the functions of HREs located in the putative promoter region from -1884 to -217 which includes three potential HREs (HRE1, -2, and -3) in K562 erythroleukemia cells, an easy cellular model for chromatin preparation. As with the other two cell lines, elevated protein levels of HIF-1 α and FtMt were observed when K562 cells were exposed to 1% O₂ for 14 h (Fig 4D and 4E). By ChIP assay, we found another functional HRE (named HRE1 here) that can bind to HIF-1 α in cells treated with 1% O₂. In contrast, HRE2 and HRE3 did not exhibit HIF-1 α binding activity (Fig 4F). Taken together, our results show that HIF-1 α protein, in response to hypoxia, transcriptionally enhances human *FTMT* expression through HREs located in the gene's promoter region (Fig 4G).

Hypoxia-induced brain cell death is attenuated by overexpression of FtMt.

It is well-known that hypoxia can induce cell damage, however little has been described about the relationship between FtMt and hypoxia-induced impairment in the brain. We used *Ftmt*^{-/-} mice to study the effects of hypoxia on cell injury in the hippocampus and cortex of mice. After continuous hypobaric hypoxia, we confirmed an increase in the levels of HIF-1 α in mice hippocampi (Fig 5A, 5B). In the mouse hippocampus, hypoxia also induced marked cell death, which was exacerbated by the absence of FtMt (approx. two folds' increase, Fig 5C and 5D). In the mouse cortex, FtMt knockout can also worsen hypoxia induced cell death (Fig 53).

We further investigated the protective effects of FtMt in a fly model. To achieve overexpression of FtMt in the *Drosophila* nervous system, we crossed the transgenic (*Fer3HCH*, expressing the orthologous human *FTMT*) lines with the *elav-Gal4* (nerve system expressing) driver line. As a control, we crossed a strain lacking the transgenes of the same genetic background. After 5% O₂ treatment, we observed a significantly higher death rate in the control group compared to the FtMt overexpressing animals (Fig 5E).

To validate this data in a human cell model, we exposed a neuroblastoma cell line, SH-SY5Y, stably overexpressing FtMt (FtMt-SY5Y(45)) to hypoxia. In addition, we further detected the endogenous expression of human FtMt using our mouse anti-human

10

monoclonal antibody (24), K562 Mt6 was used as a positive control (Fig 6A). In a cell viability assay, control cells (pcDNA3.1-SY5Y) showed a significant, ~50%, decrease after a 1% O₂ treatment, while the FtMt-SY5Y cells showed only a slightly reduced cell viability (Fig 6B). We confirmed this result using the Annexin V/PI staining method to detect apoptotic cells (Fig 6C-6D). These results demonstrate that FtMt has an indispensable role in preventing cell death in conditions of low oxygen.

FtMt inhibits Caspase 3-dependent apoptosis and blocks iron-dependent oxidative stress.

To further investigate the apoptotic pathway induced by hypoxia, *Ftmt*^{-/-} mice were placed into the hypoxic chamber for 18 h hypobaric hypoxia, after which apoptosis-related proteins were assayed. The ratio of Bcl-2/Bax dropped dramatically in the WT HH group compared to the WT Control group. However, the Bcl-2/Bax ratio decreased even more in the *Ftmt*^{-/-} HH group (KO HH). We found the same trend in the cleavage of Caspase 3, indicating that a lack of *Ftmt* may lead to severe neuronal apoptosis in the mouse brain (Fig 7A-C) (see also Fig S4). In *in vitro* experiments, hypoxia-exposed pcDNA3.1-SY5Y cells presented signs of apoptosis both through a decreased ratio of Bcl-2/Bax and increased cleavage of Caspase 3 (Fig 7D-F), while in the hypoxic FtMt-SY5Y, the ratio of Bcl-2/Bax was increased compared to the hypoxic pcDNA3.1-SY5Y cells. Additionally, the hypoxic FtMt overexpressing cells exhibited lower Caspase 3 activation compared to hypoxic controls (Fig 7D-F).

Using the calcein-AM method (see Methods), we detected a remarkably high level of cellular chelatable iron after hypoxia treatment (Fig 7G). As expected, overexpression of FtMt reduced this chelatable iron level, thus maintaining the cytosolic free iron pool within a “safe” range. The role of hypoxia in increasing intracellular ROS levels is well established (5,39). As expected, the level of ROS, as reflected by the DCFH-DA fluorescence level, was increased in pcDNA3.1-SY5Y cells under hypoxia. Again, FtMt exerted protective effects in these experiments, with the FtMt-SY5Y cells exhibiting lower DCFH-DA fluorescence levels under hypoxia (Fig 7H). To test whether FtMt has a protective role in mitochondria, we estimated mitochondrial membrane potential (MMP) by assaying the mitochondrial

retention of rhodamine 123 in living cells, as previously described (45). In pcDNA3.1-SY5Y cells treated for 24 h with 1% O₂, MMP was significantly decreased compared to untreated cells; this trend was weakened in FtMt-SY5Y cells (Fig 7I). Moreover, the MMP was preserved in hypoxia-treated FtMt-SY5Y cells, providing additional evidence of FtMt's protective role in mitochondria.

Discussion

The preferential expression of FtMt in cell types with vigorous metabolic activity and high oxygen consumption inspired us to ask if *FTMT* may be a HIF-1 α target gene. For the first time, we show that FtMt expression was increased by both hypoxia and in chemically-mimicked (CoCl₂) hypoxia. In the nervous system, this increase in FtMt is accompanied by the activation of HIF-1 α both *in vitro* and *in vivo*. Recently published data characterized the human *FTMT* promoter, revealing the existence of one positive and one negative regulatory region with a minimal promoter region located in the 500 bp upstream of the TSS (17). In the same study, CREB, a binding site of which we have shown is located near the predicted HRE1 sequence in our study (the green frame in Fig 3B), was identified as a transcription factor (TF) that binds to the positive regulatory region in the human *FTMT* promoter (17). Another study also showed that CREB acts as one of the TFs involved in hypoxia transcriptional progress (13). Here we add new information on the regulation of *FTMT* with the identification and functional characterization of HREs in the *FTMT* promoter. By sequence alignment, we found very high similarities among human, macaque and chimpanzee in the DNA sequence 2000 bp upstream of the TSS (> 90%). Among the 6 HREs identified and analyzed, HRE1, -4 and -6 were fully conserved among the three species. In the 3'-deletion DLR assays, as opposed to the -1884/-874 deletion, which contains none of the putative HREs, the -1884/-777 construct containing only HRE1 had the highest luciferase activity when the HeLa cells were exposed to 1% O₂. Importantly, the -1884/-521 deletion exhibited the lowest luciferase activities in the normoxia condition, which is in support of the existence of a negative regulatory region in the promoter about 500 bp upstream of the TSS as previously reported (17). Nonetheless, increased expression in this construct can be still activated by incubation at 1% O₂. CHIP assays probing for the HRE1, HRE2 and HRE3 sequences showed that, in this more distal promoter region from -

1884 to -217 upstream of the TSS, only HRE1, located in the positive regulatory region, possesses HIF-1 α binding activity. Collectively, our data prove that the expression of FtMt is hypoxia-inducible and, in a hypoxic environment, stabilized HIF-1 α can bind to the HREs located in the positive regulatory and minimal promoter regions of human *FTMT* (Fig 4G). FtMt protein levels changed together with the mRNA regulation. Our research provides a fresh view of the human *FTMT* promoter and highlights the mechanisms of *FTMT* regulation under hypoxia, which is congruent with an importance of FtMt in cell types of high oxygen consumption.

A recent study examining FtMt expression in hypoxia showed that the FtMt protein decreases after 48 h hypoxia in human ARPE-19 cells, without alterations in *Ftmt* mRNA levels (57). This may indicate that there are altered regulatory mechanisms in different cell types. In the same study, it was revealed that FtMt overexpression in ARPE-19 cells can stabilize HIF-1 α protein under normoxia. Thus, an interesting regulatory loop may exist between FtMt and HIF-1 α regulation. We speculate that FtMt overexpression can cause iron deprivation in the cytosol and subsequently decrease intracellular iron availability, which is a critical cofactor in prolyl hydroxylase domain (PHD) enzymes. This inhibition of PHD maturation would thereby block HIF-1 α degradation. Our hypothesis is supported by a publication in which lipopolysaccharide (LPS) induces ferritin expression and lowers free available iron levels. This results in the deprivation of the essential PHD cofactor and HIF-1 α stabilization in normal oxygen conditions (47). However, the detailed regulatory mechanisms still needed clarification in physiologically representative systems.

The induction of apoptosis by hypoxia has been revealed in numerous studies: hypoxic exposure of primary oligodendrocytes resulted in increased iron content and ROS levels (38); both apoptotic and necrotic cell death induced by intermittent hypoxia were observed in primary cultures of cerebellar granule cells (10). In addition, the energy decline accompanying hypoxia and deprivation of metabolic substrates was shown to predispose rat kidney proximal tubule cells to injury (40); loss of mitochondrial respiration and lethal cell injury in the ischemic myocardium has been detected during *in vivo* ischemia and hypoxic perfusion of hearts (33,40,64). In our study, we confirmed that hypoxia can increase brain cell death *in vivo* (in the mouse brain and in *Drosophila*) and *in vitro* (in SH-SY5Y cells).

A high metabolic rate is a common characteristic between tissues with high FtMt expression (41) (brain, heart and kidney) and tissues sensitive to hypoxic injury. We therefore hypothesized that an increased expression of FtMt during hypoxia may be a response to avoid tissue damage derived from oxygen limitation. To prove our hypothesis, we used *Ftmt*^{-/-} mice and FtMt-overexpressing SH-SY5Y cells and found that in *Ftmt*^{-/-} mice, cell death caused by hypoxia was more severe while the overexpression of FtMt in SH-SY5Y cells significantly lessened the effects of hypoxia. Furthermore, our findings in *Drosophila* overexpressing FtMt only in nervous system, suggest that hypoxia induced fly death seemed genotype dependent and gender-specific since: i) all the flies showed a higher death rate after hypoxia that was decreased by overexpression of Fer3HCH; ii) both WT and Fer3HCH-overexpressing female flies exhibited higher survival ability than males in low oxygen conditions. The latter finding is consistent with a previous study which reported that Fer3HCH overexpression improves resistance to paraquat toxicity in female flies (32). Collectively, our data shows that FtMt has a neuroprotective role in the context of hypoxia-induced brain cell death.

A sequence of events leads to apoptosis during prolonged or severe hypoxia. This cascade requires the release of anti- and pro-apoptotic proteins, such as the apoptotic effector Bax, Caspase 3 and Bcl-2 (16,37). In our study, we observed the pro-apoptotic duo of a decreased ratio of Bcl2/Bax and increased cleavage of Caspase 3 under hypoxia in both WT mice and in cells. This condition worsened with disruption of *Ftmt* in mice, and was abrogated with FtMt overexpression in SH-SY5Y cells.

Several reports demonstrate that ROS levels increase under hypoxic conditions, leading to programmed cell death (16,22,23,36). We speculated that FtMt functions as a ROS scavenger during hypoxic injury in our cell model since FtMt can sequester iron from the cytosol in mitochondria (2). We observed elevated levels of ROS accompanied by elevated amounts of chelatable iron and decreased mitochondrial membrane potential (MMP) in pcDNA3.1-SY5Y cells after hypoxia. In addition, the elevated level of TfR1 expression during hypoxia can also result in increasing iron uptake into cells, which could be one of the resource of the increased chelatable iron in our cell model (30). All of these were significantly rescued by the overexpression of FtMt. In light of this finding, we tentatively put forward a working model in which hypoxia increases uncommitted iron

that, left unchecked, can stimulate ROS-derived mitochondrial dysfunction, leading to apoptosis. In this model, FtMt has a primary role of iron detoxification in cell types of high oxygen-consumption where iron sequestration is needed to decrease the catalytic iron-derived ROS toxicity under oxygen limitation. This may partially explain the extremely low level of FtMt in most solid tumor cell lines. In contrast to non-neoplastic cells in which severe hypoxia or anoxia initiates a cascade of events that leads to apoptosis that may be prevented by FtMt function, in solid tumors, the tissue has acclimated to hypoxia, having selected cells that are resistant to hypoxia and not as dependent on mitochondrial oxidative phosphorylation. Under these circumstances, FtMt may not be needed to mitigate iron-catalyzed ROS because the hypoxic resistance occurs through other mechanisms. This idea is supported by previous studies in which FtMt overexpression stunted *in vivo* tumor growth (34,46).

In summary, our current study demonstrates that the expression of FtMt is regulated by HIF-1 α in hypoxia; *FTMT* is a novel HIF-1 α target that plays a neuroprotective role in the oxidative damage-induced cell death caused by hypoxia through reducing the ROS caused by elevated uncommitted iron levels in cells. Our findings not only offer an explanation for why FtMt levels are sustained in tachyaerobic organs but also may provide a therapeutic approach to diseases characterized by oxygen deprivation, as ischemic stroke.

Innovation

Hypoxia is a paradigm of responses involving the whole organism. The function and regulation of mitochondrial ferritin has remained elusive. Our study describes the first functional regulatory axis with mitochondrial ferritin as the effector activating the hypoxia transcriptional program in oxygen deficiency. Mitochondrial ferritin is a novel HIF-1 α target gene. This finding that the protein eliminates the high oxidative stress resulting from hypoxia highlights the causes underlying FtMt's peculiar expression pattern. Furthermore, our results point to mitochondrial ferritin as a potential therapeutic target in situations of hypoxic challenge such as ischemic stroke.

Methods

In silico human *FTMT* promoter experiments

The *FTMT* 5' evolutionarily conserved region alignments between human, mouse, rat, rhesus macaque and chimpanzee were performed using the ECR Browser according to the instructions in the official website and Clustal Omega(29). The transcription binding sites and prediction of the transcription factors were analyzed by MatInspector (Genomatix Software GmbH) (7), PROMO (14) and by TFBIND (51).

Materials

Dulbecco's modified Eagle's medium (DMEM), Modified Eagle's medium (MEM) and fetal calf serum were purchased from Gibco BRL (Grand Island, NY, USA). The *In Situ* Cell Death Detection Kit, Fluorescein was purchased from Roche (Mannheim, Germany). Annexin V/PI, rhodamine 123, calcein-AM, anti- β -actin antibody and 2,7-dichlorofluorescein diacetate (DCFH-DA) were purchased from Sigma (St. Louis, MO USA). MTT, TRIzol reagent, Lipofectamine 2000, and rat *FtMt* siRNA were purchased from Invitrogen. Anti-Bcl-2 and anti-Bax antibodies were purchased from Santa Cruz Biotechnology. The anti-HIF-1 α antibody and anti-TIM44 antibody were obtained from Novus Biologicals (Littleton, CO, USA). Antibodies to Caspase 3 and Cleaved-Caspase 3 were purchased from Cell Signaling Technology. The anti-*FtMt* antibody was homemade as described in our previous publication (41).

Animals and hypobaric hypoxia (HH) treatment

Adult male C57BL/6J and *Ftmt*^{-/-} mice were housed in stainless steel rust-free cages at 22–24°C with 45–55% relative humidity. All animals were provided free access to food and water. All experiments were approved by the institutional Animal Care and Use Committee (Hebei Normal University, Shijiazhuang, China). The animals were placed in a hypobaric chamber (Guizhou Fenglei, China) in our lab. The chamber can imitate hypobaric hypoxia; the simulated altitude (8000 m) was selected based on trials and previous reports (27,44,68) to create hypoxic conditions in the chamber at a velocity of approximately 20 m/s, the O₂ content in the altitude 8000 m is around 8.5% (O₂ content was 20% in the control group) and the hypoxia exposure time was 18 h. For *Drosophila* maintenance, the

procedures were as described previously (46), the O₂ content for the *Drosophila* was 5% for 18 h.

Cell culture and hypoxic treatment

The C6 and HeLa cell lines were maintained in DMEM; U251 cells were cultured in MEM; the human erythroleukemic K562 cells were cultured in RPMI (Lonza, Basel, Switzerland), all the cells were supplemented with 10% fetal calf serum and 100 U/ml penicillin/streptomycin at 37°C and 5% CO₂. FtMt-overexpression (FtMt-SY5Y) cells and pcDNA3.1-SY5Y cells were obtained and cultured as previously described (45). The hypoxia treatment for all the cell lines was 1% O₂, 5% CO₂ and 94% N₂. For CoCl₂ treatments, the CoCl₂ was dissolved in sterile H₂O and the cells were treated for the indicated time periods.

Immunoblotting, reverse transcription-PCR analysis and quantitative real-time PCR analysis

For detecting normal protein expression, immunoblotting was performed as previously described (46). For HIF-1 α protein detection, PE-lysis buffer (6.65 M urea, 10% glycerol, 1% SDS, Tris [tris(hydroxymethyl)aminomethane] HCl, pH 6.8, 5 mM DTT) was used to generate cell lysates according to methods described previously (47). Total RNA was extracted from cultured cells or tissues using TRIzol reagent according to the manufacturer's instructions. 1 μ g total RNA was reverse transcribed for reverse transcription-PCR (45) or quantitative real-time PCR (qRT-PCR) with an ABI 7900HT Fast Real Time PCR System (Applied Biosystems) using SYBR[®] Green Real-Time PCR Master Mix (Applied Biosystems). The primer sequences used are listed in Table 2. Data were analyzed using the $\Delta\Delta C_T$ method. The normalized ratio of target mRNA to the internal control mRNA β -actin (*Actb*) was set to 1. The relative band intensities of the proteins are expressed as the ratio of each to β -actin.

Detection of apoptosis in cultured cells and in mouse brain

Under anesthesia with 0.4% Nembutal, the mice were sacrificed, the brains were then removed, post-fixed for 72-96 h and then stored overnight in 30% sucrose. Serial coronal sections were cut at a thickness of 15 μ m on a freezing microtome (Leica CM1950) and mounted onto a slide covered with APES (Beijing ZhongShan Biotechnology, Beijing, China). The presence of apoptosis in the mouse cortex and hippocampus regions after HH treatment was assessed by the terminal deoxynucleotidyl transferase-mediated Cyanine 3 (Cy 3) -dUDP nick-end labeling method using the One Step TUNEL Apoptosis Assay Kit (Beyotime Biotechnology, Shanghai, China) following the manufacturer's protocol. Apoptosis in SH-SY5Y cells was measured by flow cytometry using Annexin V/PI staining as previously described (45).

Double Immunofluorescence

The brain slices were washed three times with 0.01 M PBS. Antigen retrieval was performed in a microwave oven for 10 min in 10 mM citrate buffer (pH 6.0). After blocking for 1 h with normal goat serum prepared in 0.01 M PBS, the slices were incubated overnight at 4°C with the mouse anti-NeuN monoclonal antibody (1:100; ab104224, Abcam, Abcam Trading [Shanghai] Company Ltd), mouse anti-GFAP monoclonal antibody (1:500; Millipore Corporation, Temecula, CA), mouse anti-Iba1 monoclonal antibody (1:200; Millipore Corporation, Temecula, CA) and mouse anti-COX IV monoclonal antibody (1:200; ab14744, Abcam, Abcam Trading [Shanghai] Company Ltd), and FtMt antibody (1:200). The slides were then washed three times for 5 min with 0.01 M PBS. The following secondary antibodies were used in 50 min incubations at 37°C: DyLight 549, goat anti-rabbit IgG (1:200; Abbkine Scientific Co., Ltd., Wuhan, China) and DyLight 488, goat anti-mouse IgG (1:200; Abbkine Scientific Co., Ltd., Wuhan, China). Finally, after washing and mounting, the sections were analyzed with an OLYMPUS FV3000 Confocal Laser Scanning Microscope.

Transfection and Dual Luciferase Reporter (DLR) assay

The plasmids for 3' deletion (-1884/-874, -1884/-777, -1884/-521, -1884/-217) and 5' deletion (-902/+9, -491/+9, -217/+9) of the *FTMT* promoter were as previously

described(17). HeLa cells were seeded in 48-well plates, grown to 90% confluence before transfection and maintained in ambient air (20% O₂). A Dual-Luciferase-Reporter System (Promega and Abnova) was used. Cells were transiently transfected with pGL2-Basic (mock) or reporter constructs (0.4 µg) accompanied by Renilla luciferase (Rluc) control reporter vectors pRL-TK (20 ng). Transient transfection was performed using Lipofectamine 2000 (Invitrogen) according to the manufacturer's protocol. After 1% O₂ treatment, cells were harvested and the luciferase activity was quantitated using a Victor 3 1420 Multilabel Counter (Perkin Elmer). The firefly luciferase activity was normalized to the control, Renilla luciferase activity.

Electrophoretic mobility shift assay (EMSA) and Chromatin Immunoprecipitation (ChIP)

Nuclear extracts from U251 cells were used for EMSA. The biotin-labeled and unlabeled double-stranded oligonucleotide probes containing HIF-1 α binding sites (hypoxia response element, HRE) were synthesized by Invitrogen. Nuclear extracts, biotin-labeled probe, 10 \times binding buffer (100 mM Tris, 500 mM KCl, 10 mM DTT, pH 7.5), 1% NP-40, 50% Glycerol, 100 mM MgCl₂ and Poly(dI·dC) were combined in 20 µl, and incubated for 20 min at room temperature. The EMSA was performed following the protocol of the LightShift Chemiluminescent EMSA kit (Thermo Fisher).

The ChIP experiments were performed according to a previously reported method (17). The HIF-1 alpha Antibody (NB100-134) from Novus Biologicals (Littleton, CO, USA) was used. Specific primers used to detect the amplified human *FTMT* promoter region are provided in Table S2.

Measurement of intracellular ROS, MMP and chelatable iron.

The level of ROS in pcDNA3.1-SY5Y and FtMt-SY5Y cells was quantified by assessing the fluorescence of DCFH-DA according to the methods of Bass *et al*(4). Changes in MMP were analyzed by calculating the retention of rhodamine 123 as previously described (45). Chelatable iron levels in pcDNA3.1-SY5Y and FtMt-SY5Y cells were measured according to methods in the literature (45). For these studies, the cells were treated with 1% O₂ for 24 h.

Statistical Analysis

Results are expressed as means \pm SD. If not indicated otherwise, n represents biological samples obtained from N independent experiments or mice. Data were analyzed using Prism v5.0 (GraphPad Software). In general, for normally distributed data, two tailed unpaired Student's *t*-test or analysis of variance was used. A *p*-value < 0.05 was considered statistically significant.

Acknowledgements

This work was supported by the National Natural Science Foundation of China (grant numbers 31520103908, 31471035, 31300898, 31271473) and by scholarships from the China Scholarship Council (CSC) awarded to Q.W. The authors wish to thank Alex Sheftel (High Impact Editing) for language editing and critical reading.

Author Disclosure Statement

The authors declare that they have no conflict of interest.

List of Abbreviations

AD = Alzheimer's disease;

Bax = Bcl-2 Associated X protein;

Bcl-2 = B-cell lymphoma-2;

ChIP = Chromatin immunoprecipitation;

DLR = Dual-luciferase reporter assay;

FtMt (protein), *FTMT* (gene symbol, human), *Ftmt* (gene symbol, mouse and rat) = mitochondrial ferritin;

HIF-1 α = hypoxia inducible factor-1;

HRE = hypoxia-responsive element;

MMP = mitochondria membrane potential;

PD = Parkinson's disease;

qRT-PCR = quantitative real time PCR;

RLS = restless legs syndrome;

ROS = Reactive Oxygen Species;

RT-PCR = reverse transcription-PCR;

SDS-PAGE = SDS polyacrylamide gel electrophoresis;

TUNEL = terminal deoxynucleotidyl transferase-mediated dUTP-biotin nick-end labeling assay;

TfR = transferrin receptor;

YC-1 = 3-(5'-hydroxymethyl-2'-furyl)-1-benzylindazole;

References

1. Agani F, Semenza GL. Mersalyl is a novel inducer of vascular endothelial growth factor gene expression and hypoxia-inducible factor 1 activity. *Mol Pharmacol* 54: 749-54, 1998.
2. Arosio P, Levi S. Cytosolic and mitochondrial ferritins in the regulation of cellular iron homeostasis and oxidative damage. *Biochim Biophys Acta* 1800: 783-92, 2010.
3. Badawi Y, Ramamoorthy P, Shi H. Hypoxia-inducible factor 1 protects hypoxic astrocytes against glutamate toxicity. *ASN Neuro* 4: 231-41, 2012.
4. Bass DA, Parce JW, Dechatelet LR, Szejda P, Seeds MC, Thomas M. Flow cytometric studies of oxidative product formation by neutrophils: a graded response to membrane stimulation. *J Immunol* 130: 1910-7, 1983.
5. Bullova P, Cougnoux A, Abunimer L, Kopacek J, Pastorekova S, Pacak K. Hypoxia potentiates the cytotoxic effect of piperlongumine in pheochromocytoma models. *Oncotarget* 7: 40531-40545, 2016.
6. Campanella A, Rovelli E, Santambrogio P, Cozzi A, Taroni F, Levi S. Mitochondrial ferritin limits oxidative damage regulating mitochondrial iron availability: hypothesis for a protective role in Friedreich ataxia. *Hum Mol Genet* 18: 1-11, 2009.
7. Cartharius K, Frech K, Grote K, Klocke B, Haltmeier M, Klingenhoff A, Frisch M, Bayerlein M, Werner T. MatInspector and beyond: promoter analysis based on transcription factor binding sites. *Bioinformatics* 21: 2933-42, 2005.
8. Castiglioni E, Finazzi D, Goldwurm S, Levi S, Pezzoli G, Garavaglia B, Nardocci N, Malcovati L, Porta MG, Galli A, Forni GL, Girelli D, Maccarinelli F, Poli M, Ferrari M, Cremonesi L, Arosio P. Sequence variations in mitochondrial ferritin: distribution in healthy controls and different types of patients. *Genet Test Mol Biomarkers* 14: 793-6, 2010.
9. Cazzola M, Invernizzi R, Bergamaschi G, Levi S, Corsi B, Travaglino E, Rolandi V, Biasiotto G, Drysdale J, Arosio P. Mitochondrial ferritin expression in erythroid cells from patients with sideroblastic anemia. *Blood* 101: 1996-2000, 2003.
10. Chiu SC, Huang SY, Tsai YC, Chen SP, Pang CY, Lien CF, Lin YJ, Yang KT. Poly (ADP-ribose) polymerase plays an important role in intermittent hypoxia-induced cell death in rat cerebellar granule cells. *J Biomed Sci* 19: 29, 2012.

11. Corsi B, Cozzi A, Arosio P, Drysdale J, Santambrogio P, Campanella A, Biasiotto G, Albertini A, Levi S. Human mitochondrial ferritin expressed in HeLa cells incorporates iron and affects cellular iron metabolism. *J Biol Chem* 277: 22430-7, 2002.
12. Drysdale J, Arosio P, Invernizzi R, Cazzola M, Volz A, Corsi B, Biasiotto G, Levi S. Mitochondrial ferritin: a new player in iron metabolism. *Blood Cells Mol Dis* 29: 376-83, 2002.
13. Ebert BL, Bunn HF. Regulation of transcription by hypoxia requires a multiprotein complex that includes hypoxia-inducible factor 1, an adjacent transcription factor, and p300/CREB binding protein. *Mol Cell Biol* 18: 4089-96, 1998.
14. Farre D, Roset R, Huerta M, Adsuara JE, Rosello L, Alba MM, Messeguer X. Identification of patterns in biological sequences at the ALGGEN server: PROMO and MALGEN. *Nucleic Acids Res* 31: 3651-3, 2003.
15. Galatro A, Puntarulo S. Mitochondrial ferritin in animals and plants. *Front Biosci* 12: 1063-71, 2007.
16. Greijer AE, van der Wall E. The role of hypoxia inducible factor 1 (HIF-1) in hypoxia induced apoptosis. *J Clin Pathol* 57: 1009-14, 2004.
17. Guaraldo M, Santambrogio P, Rovelli E, Di Savino A, Saglio G, Cittaro D, Roetto A, Levi S. Characterization of human mitochondrial ferritin promoter: identification of transcription factors and evidences of epigenetic control. *Sci Rep* 6: 33432, 2016.
18. Ho VT, Bunn HF. Effects of transition metals on the expression of the erythropoietin gene: further evidence that the oxygen sensor is a heme protein. *Biochem Biophys Res Commun* 223: 175-80, 1996.
19. Hota SK, Barhwal K, Singh SB, Ilavazhagan G. Differential temporal response of hippocampus, cortex and cerebellum to hypobaric hypoxia: a biochemical approach. *Neurochem Int* 51: 384-90, 2007.
20. Iyer NV, Kotch LE, Agani F, Leung SW, Laughner E, Wenger RH, Gassmann M, Gearhart JD, Lawler AM, Yu AY, Semenza GL. Cellular and developmental control of O₂ homeostasis by hypoxia-inducible factor 1 alpha. *Genes Dev* 12: 149-62, 1998.

21. Jain IH, Zazzeron L, Goli R, Alexa K, Schatzman-Bone S, Dhillon H, Goldberger O, Peng J, Shalem O, Sanjana NE, Zhang F, Goessling W, Zapol WM, Mootha VK. Hypoxia as a therapy for mitochondrial disease. *Science* 352: 54-61, 2016.
22. Kim JW, Tchernyshyov I, Semenza GL, Dang CV. HIF-1-mediated expression of pyruvate dehydrogenase kinase: a metabolic switch required for cellular adaptation to hypoxia. *Cell Metab* 3: 177-85, 2006.
23. Kim JY, Park JH. ROS-dependent caspase-9 activation in hypoxic cell death. *FEBS Lett* 549: 94-8, 2003.
24. Koeppen AH, Ramirez RL, Becker AB, Bjork ST, Levi S, Santambrogio P, Parsons PJ, Kruger PC, Yang KX, Feustel PJ, Mazurkiewicz JE. The pathogenesis of cardiomyopathy in Friedreich ataxia. *PLoS One* 10: e0116396, 2015.
25. Langlois d'Estaintot B, Santambrogio P, Granier T, Gallois B, Chevalier JM, Precigoux G, Levi S, Arosio P. Crystal structure and biochemical properties of the human mitochondrial ferritin and its mutant Ser144Ala. *J Mol Biol* 340: 277-93, 2004.
26. Levi S, Corsi B, Bosisio M, Invernizzi R, Volz A, Sanford D, Arosio P, Drysdale J. A human mitochondrial ferritin encoded by an intronless gene. *J Biol Chem* 276: 24437-40, 2001.
27. Li MM, Wu LY, Zhao T, Wu KW, Xiong L, Zhu LL, Fan M. The protective role of 5-hydroxymethyl-2-furfural (5-HMF) against acute hypobaric hypoxia. *Cell Stress Chaperones* 16: 529-37, 2011.
28. Li SH, Shin DH, Chun YS, Lee MK, Kim MS, Park JW. A novel mode of action of YC-1 in HIF inhibition: stimulation of FIH-dependent p300 dissociation from HIF-1{alpha}. *Mol Cancer Ther* 7: 3729-38, 2008.
29. Li W, Cowley A, Uludag M, Gur T, McWilliam H, Squizzato S, Park YM, Buso N, Lopez R. The EMBL-EBI bioinformatics web and programmatic tools framework. *Nucleic Acids Res* 43: W580-4, 2015.
30. Lok CN, Ponka P. Identification of a hypoxia response element in the transferrin receptor gene. *J Biol Chem* 274: 24147-52, 1999.
31. Lu Z, Nie G, Li Y, Soe-Lin S, Tao Y, Cao Y, Zhang Z, Liu N, Ponka P, Zhao B. Overexpression of mitochondrial ferritin sensitizes cells to oxidative stress via an iron-mediated mechanism. *Antioxid Redox Signal* 11: 1791-803, 2009.

32. Missirlis F, Holmberg S, Georgieva T, Dunkov BC, Rouault TA, Law JH. Characterization of mitochondrial ferritin in *Drosophila*. *Proc Natl Acad Sci U S A* 103: 5893-8, 2006.
33. Murry CE, Jennings RB, Reimer KA. Preconditioning with ischemia: a delay of lethal cell injury in ischemic myocardium. *Circulation* 74: 1124-36, 1986.
34. Nie G, Chen G, Sheftel AD, Pantopoulos K, Ponka P. In vivo tumor growth is inhibited by cytosolic iron deprivation caused by the expression of mitochondrial ferritin. *Blood* 108: 2428-34, 2006.
35. Nie G, Sheftel AD, Kim SF, Ponka P. Overexpression of mitochondrial ferritin causes cytosolic iron depletion and changes cellular iron homeostasis. *Blood* 105: 2161-7, 2005.
36. Peng C, Rao W, Zhang L, Wang K, Hui H, Wang L, Su N, Luo P, Hao YL, Tu Y, Zhang S, Fei Z. Mitofusin 2 ameliorates hypoxia-induced apoptosis via mitochondrial function and signaling pathways. *Int J Biochem Cell Biol* 69: 29-40, 2015.
37. Piret JP, Mottet D, Raes M, Michiels C. Is HIF-1alpha a pro- or an anti-apoptotic protein? *Biochem Pharmacol* 64: 889-92, 2002.
38. Rathnasamy G, Murugan M, Ling EA, Kaur C. Hypoxia-Induced Iron Accumulation in Oligodendrocytes Mediates Apoptosis by Eliciting Endoplasmic Reticulum Stress. *Mol Neurobiol*: 1-15, 2015.
39. Sabharwal SS, Schumacker PT. Mitochondrial ROS in cancer: initiators, amplifiers or an Achilles' heel? *Nat Rev Cancer* 14: 709-21, 2014.
40. Saikumar P, Dong Z, Patel Y, Hall K, Hopfer U, Weinberg JM, Venkatachalam MA. Role of hypoxia-induced Bax translocation and cytochrome c release in reoxygenation injury. *Oncogene* 17: 3401-15, 1998.
41. Santambrogio P, Biasiotto G, Sanvito F, Olivieri S, Arosio P, Levi S. Mitochondrial ferritin expression in adult mouse tissues. *J Histochem Cytochem* 55: 1129-37, 2007.
42. Santambrogio P, Erba BG, Campanella A, Cozzi A, Causarano V, Cremonesi L, Galli A, Della Porta MG, Invernizzi R, Levi S. Over-expression of mitochondrial ferritin affects the JAK2/STAT5 pathway in K562 cells and causes mitochondrial iron accumulation. *Haematologica* 96: 1424-32, 2011.

43. Semenza GL. Transcriptional regulation by hypoxia-inducible factor 1 molecular mechanisms of oxygen homeostasis. *Trends Cardiovasc Med* 6: 151-7, 1996.
44. Sharma NK, Sethy NK, Bhargava K. Comparative proteome analysis reveals differential regulation of glycolytic and antioxidant enzymes in cortex and hippocampus exposed to short-term hypobaric hypoxia. *J Proteomics* 79: 277-98, 2013.
45. Shi ZH, Nie G, Duan XL, Rouault T, Wu WS, Ning B, Zhang N, Chang YZ, Zhao BL. Neuroprotective mechanism of mitochondrial ferritin on 6-hydroxydopamine-induced dopaminergic cell damage: implication for neuroprotection in Parkinson's disease. *Antioxid Redox Signal* 13: 783-96, 2010.
46. Shi ZH, Shi FF, Wang YQ, Sheftel AD, Nie G, Zhao YS, You LH, Gou YJ, Duan XL, Zhao BL, Xu HM, Li CY, Chang YZ. Mitochondrial ferritin, a new target for inhibiting neuronal tumor cell proliferation. *Cell Mol Life Sci* 72: 983-97, 2015.
47. Siegert I, Schodel J, Nairz M, Schatz V, Dettmer K, Dick C, Kalucka J, Franke K, Ehrenschwender M, Schley G, Beneke A, Sutter J, Moll M, Hellerbrand C, Wielockx B, Katschinski DM, Lang R, Galy B, Hentze MW, Koivunen P, Oefner PJ, Bogdan C, Weiss G, Willam C, Jantsch J. Ferritin-Mediated Iron Sequestration Stabilizes Hypoxia-Inducible Factor-1alpha upon LPS Activation in the Presence of Ample Oxygen. *Cell Rep* 13: 2048-55, 2015.
48. Snyder AM, Neely EB, Levi S, Arosio P, Connor JR. Regional and cellular distribution of mitochondrial ferritin in the mouse brain. *J Neurosci Res* 88: 3133-43, 2010.
49. Snyder AM, Wang X, Patton SM, Arosio P, Levi S, Earley CJ, Allen RP, Connor JR. Mitochondrial ferritin in the substantia nigra in restless legs syndrome. *J Neuropathol Exp Neurol* 68: 1193-9, 2009.
50. Stenirri S, Santambrogio P, Setaccioli M, Erba BG, Pia Manitto M, Rovida E, Ferrari M, Levi S, Cremonesi L. Study of FTMT and ABCA4 genes in a patient affected by age-related macular degeneration: identification and analysis of new mutations. *Clin Chem Lab Med* 50: 1021-9, 2012.
51. Tsunoda T, Takagi T. Estimating transcription factor bindability on DNA. *Bioinformatics* 15: 622-30, 1999.

52. Valko M, Jomova K, Rhodes CJ, Kuca K, Musilek K. Redox- and non-redox-metal-induced formation of free radicals and their role in human disease. *Arch Toxicol* 90: 1-37, 2016.
53. Vigani G, Tarantino D, Murgia I. Mitochondrial ferritin is a functional iron-storage protein in cucumber (*Cucumis sativus*) roots. *Front Plant Sci* 4: 316, 2013.
54. Wang GL, Jiang BH, Rue EA, Semenza GL. Hypoxia-inducible factor 1 is a basic-helix-loop-helix-PAS heterodimer regulated by cellular O₂ tension. *Proc Natl Acad Sci U S A* 92: 5510-4, 1995.
55. Wang GL, Semenza GL. Desferrioxamine induces erythropoietin gene expression and hypoxia-inducible factor 1 DNA-binding activity: implications for models of hypoxia signal transduction. *Blood* 82: 3610-5, 1993.
56. Wang L, Yang H, Zhao S, Sato H, Konishi Y, Beach TG, Abdelalim EM, Bisem NJ, Tooyama I. Expression and localization of mitochondrial ferritin mRNA in Alzheimer's disease cerebral cortex. *PLoS One* 6: e22325, 2011.
57. Wang X, Yang H, Yanagisawa D, Bellier JP, Morino K, Zhao S, Liu P, Vigers P, Tooyama I. Mitochondrial ferritin affects mitochondria by stabilizing HIF-1 α in retinal pigment epithelium: implications for the pathophysiology of age-related macular degeneration. *Neurobiol Aging* 47: 168-179, 2016.
58. Wenger RH, Gassmann M. Oxygen(es) and the hypoxia-inducible factor-1. *Biol Chem* 378: 609-16, 1997.
59. Wu W, Chang S, Wu Q, Xu Z, Wang P, Li Y, Yu P, Gao G, Shi Z, Duan X, Chang YZ. Mitochondrial ferritin protects the murine myocardium from acute exhaustive exercise injury. *Cell Death Dis* 7: e2475, 2016.
60. Wu WS, Zhao YS, Shi ZH, Chang SY, Nie GJ, Duan XL, Zhao SM, Wu Q, Yang ZL, Zhao BL, Chang YZ. Mitochondrial ferritin attenuates beta-amyloid-induced neurotoxicity: reduction in oxidative damage through the Erk/P38 mitogen-activated protein kinase pathways. *Antioxid Redox Signal* 18: 158-69, 2013.
61. Yang H, Yang M, Guan H, Liu Z, Zhao S, Takeuchi S, Yanagisawa D, Tooyama I. Mitochondrial ferritin in neurodegenerative diseases. *Neurosci Res* 77: 1-7, 2013.
62. Yang M, Yang H, Guan H, Bellier JP, Zhao S, Tooyama I. Mapping of mitochondrial ferritin in the brainstem of *Macaca fascicularis*. *Neuroscience* 328: 92-106, 2016.

63. You LH, Li Z, Duan XL, Zhao BL, Chang YZ, Shi ZH. Mitochondrial Ferritin Suppresses MPTP-induced Cell Damage by Regulating Iron Metabolism and Attenuating Oxidative Stress. *Brain Res*: 33-42, 2016.
64. Yu B, Meng F, Yang Y, Liu D, Shi K. NOX2 Antisense Attenuates Hypoxia-Induced Oxidative Stress and Apoptosis in Cardiomyocyte. *Int J Med Sci* 13: 646-52, 2016.
65. Zancani M, Peresson C, Biroccio A, Federici G, Urbani A, Murgia I, Soave C, Micali F, Vianello A, Macri F. Evidence for the presence of ferritin in plant mitochondria. *Eur J Biochem* 271: 3657-64, 2004.
66. Zanella I, Derosas M, Corrado M, Cocco E, Cavadini P, Biasiotto G, Poli M, Verardi R, Arosio P. The effects of frataxin silencing in HeLa cells are rescued by the expression of human mitochondrial ferritin. *Biochim Biophys Acta* 1782: 90-8, 2008.
67. Zhang J, Yan X, Shi J, Gong Q, Weng X, Liu Y. Structural modifications of the brain in acclimatization to high-altitude. *PLoS One* 5: e11449, 2010.
68. Zhang K, Zhao T, Huang X, Liu ZH, Xiong L, Li MM, Wu LY, Zhao YQ, Zhu LL, Fan M. Preinduction of HSP70 promotes hypoxic tolerance and facilitates acclimatization to acute hypobaric hypoxia in mouse brain. *Cell Stress Chaperones* 14: 407-15, 2009.

Table 1. Matrix Similarity of predicted HREs.

HREs \ Database	MatInspector	PROMO	TFBIND
HRE 1	0.93	0.91	0.91
HRE 2	0.90	0.91	0.72
HRE 3	0.97	Not found	Not found
HRE 4	0.95	0.90	0.78
HRE 5	0.82	0.87	0.72
HRE 6	0.92	0.87	0.88

Table 2. Primers used for reverse transcription-PCR (rat) and quantitative real time PCR (mouse).

Gene	Forward (5'-3')	Reverse (5'-3')
<i>Ftmt</i> (mouse)	AGC ACA TCA GCT CTG CAC TG	AGG CCA GTA GGG GAC CTA AA
<i>Ftmt</i> (rat)	TTA CGC ATC CTA CGT GTA CCT G	GGT TCT GCA GTC TCA TAA GCT T
<i>Actb</i> (mouse)	AGG CCC AGA GCA AGA GAG GTA	TCT CCA TGT CGT CCC AGT TG
<i>Actb</i> (rat)	GAA ATC GTG CGT GAC ATT AAA GAG	GCG GCA GTG GCC ATC TC
ChIP on HRE 1	GAG TGC AGT GGC TCG ATC T	GTG GCA GGC TGC TGT AGT
ChIP on HRE 2	CTA ACC TTG TGA TCC GCC	ATG AGA TAC TGT AGG CCG G
ChIP on HRE 3	GTA CAC TTG CTT TGG ATG TGG	GAT GCC CAG TCA CGA TTC CGT

Figure Legends

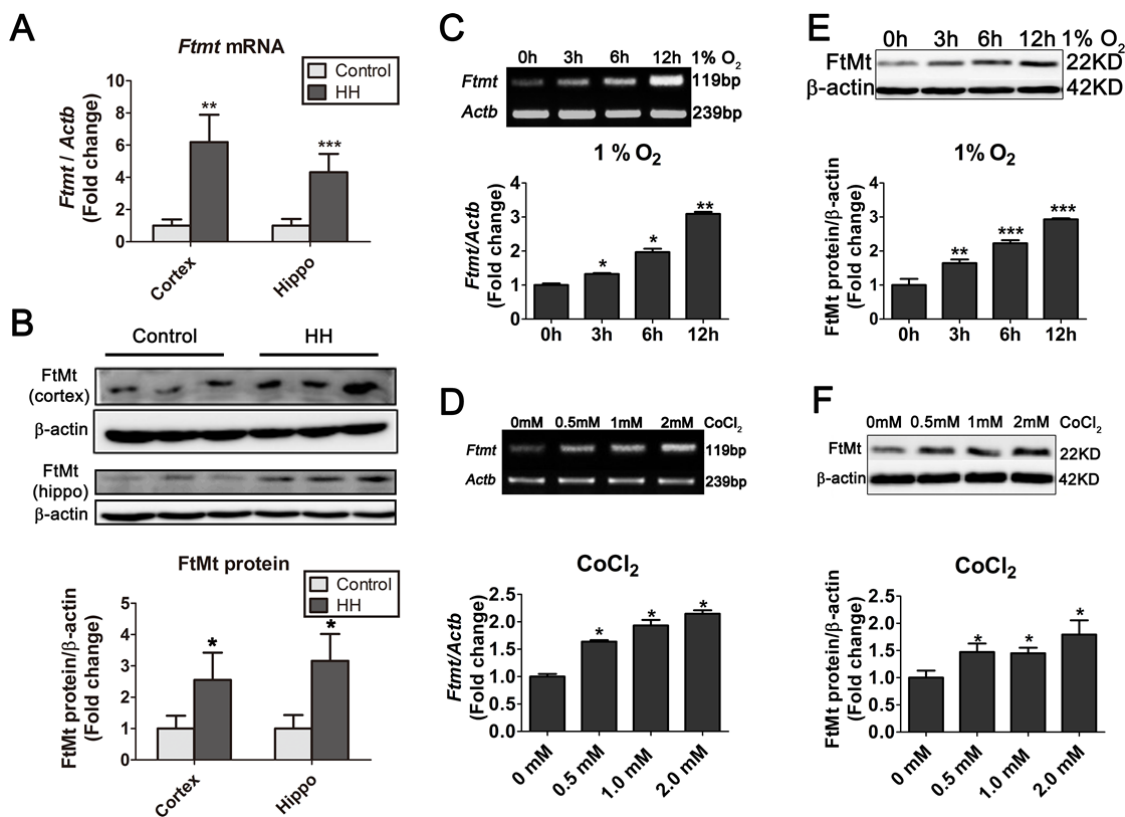


Figure 1 Mitochondrial ferritin (FtMt) increases under hypoxic conditions.

(A-B) The *Ftmt* mRNA and FtMt protein levels in the cortices and hippocampi (Hippo) of mice after 18 h continuous hypobaric hypoxia (HH). The relative expression levels of mRNA (A) and protein (B) are normalized to *Actb* / β -actin and displayed as the mean \pm SD, $n=6$. (C-D) *Ftmt* mRNA levels as measured by reverse transcription-PCR (RT-PCR) on C6 cells treated with 1% O₂ for 3, 6 and 12 h (C) or different concentrations of CoCl₂ for 12 h (D). In the RT-PCR graphs, the expression levels were normalized to *Actb* and displayed as the mean \pm SD of three independent experiments. (E-F) FtMt protein levels in C6 cells after treatment with 1% O₂ for 3, 6 and 12 h (E) or different concentrations of CoCl₂ for 12 h (F). The band densities of FtMt are normalized to β -actin and displayed as relative to the control values. Error bars show \pm SD of three independent experiments. * $p < 0.05$, ** $p < 0.01$, *** $p < 0.001$ versus the control groups (cells and animals).

Unedited blots of Figure 1B, E, and F are shown in Supplementary Western Blots (SW1)

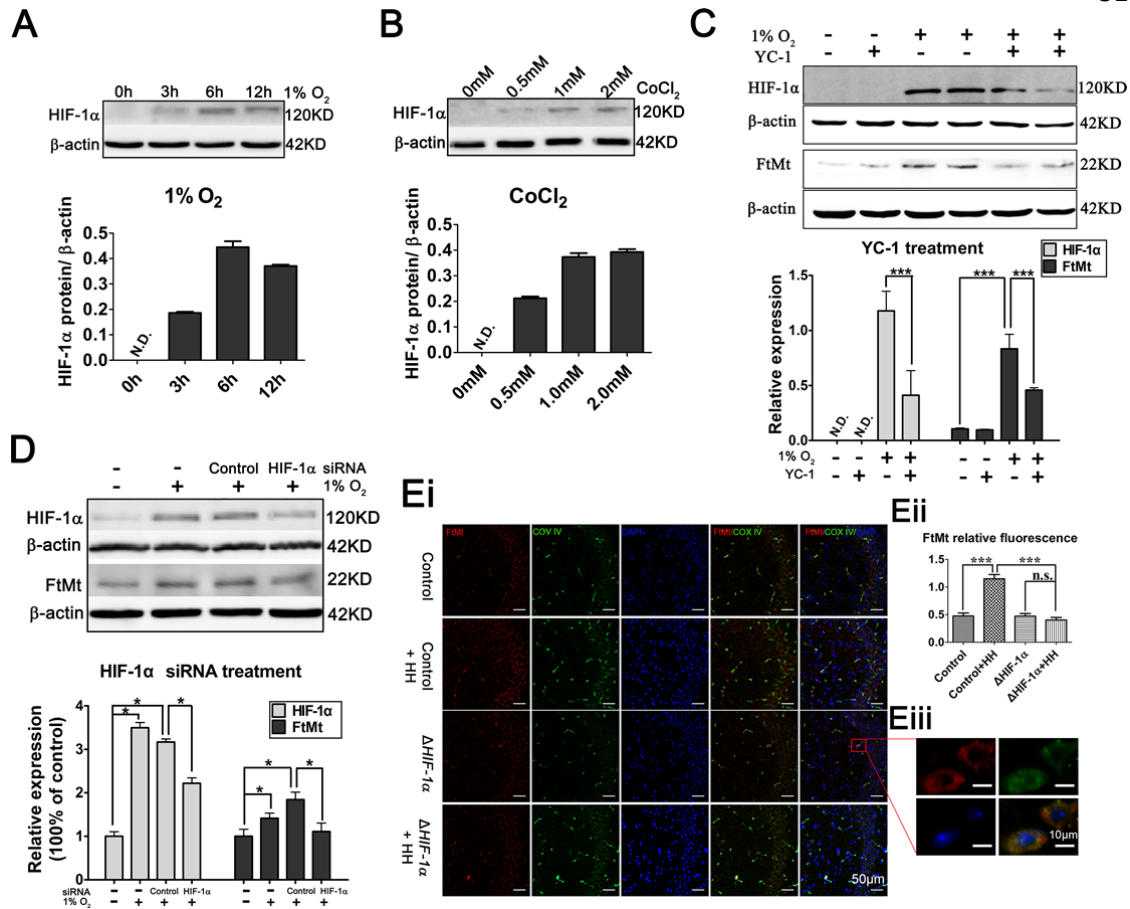


Figure 2 HIF-1 α is involved in the up-regulation of FtMt during hypoxia treatment.

(A) HIF-1 α protein levels after treatment with 1% O₂ in C6 cells, or (B) with different concentrations of CoCl₂. Data are presented relative to β -actin levels. All of the plots display the mean \pm SD of three independent experiments. (C) After treatment with the HIF-1 α inhibitor YC-1, the cells were exposed to 1% O₂ for 12 h. Whole cell lysates were collected and HIF-1 α and FtMt protein levels were examined by immunoblotting. (D) The correlation of HIF-1 α and FtMt protein after treatment with siRNA targeting HIF-1 α in C6 cells. The relative band intensities of HIF-1 α and FtMt are displayed in the lower panels of (C) and (D). Data are displayed as relative to β -actin levels. All of the plots present the mean \pm SD of three independent experiments, * p < 0.05, *** p < 0.001 versus the groups indicated. N.D., undetermined. (Ei) The expression of FtMt in HIF-1 α ^{flox/flox} mice hippocampi (Control, Control + HH groups) and conditional knock out mice (Δ HIF-1 α , Δ HIF-1 α + HH groups) are showed by double immunofluorescence with anti-FtMt (red)

and anti-COX IV antibodies (green). The FtMt relative fluorescence (**Figure 2Eii**) was measured using image J. The plots show the mean \pm SD, $n=3$, *** $p < 0.001$ versus the groups indicated; **n.s.**, not significant. Double immunostaining (**Figure 2Eiii**) with the mitochondrial marker (COX IV, green) and FtMt (red) reveals the localization of FtMt to mitochondria. Unedited blots of Figure 2A, B, C, and D are shown in Supplementary Western Blots (SW1). To see this illustration in color, the reader is referred to the online version of this article at www.liebertpub.com/ars

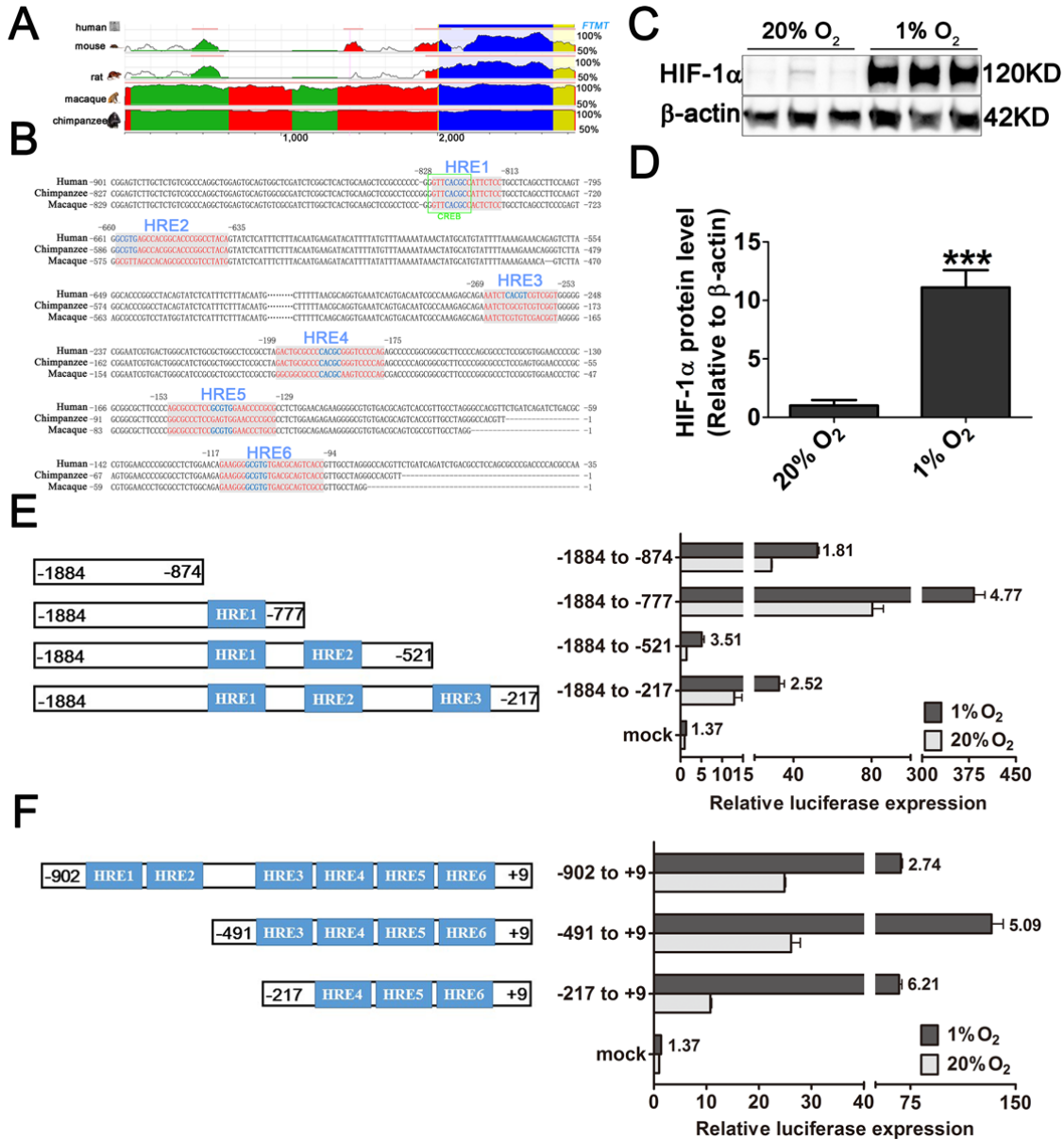


Figure 3 HIF-1 α binds to hypoxia-response-elements (HREs) located in human mitochondrial ferritin (*FTMT*) promoter to activate transcription.

(A) The *FTMT* 5' evolutionarily conserved region alignments in human, mouse, rat, rhesus macaque and chimpanzee were generated using the ECR Browser following the instructions in the website. The human *FTMT* 5' region (chr5:121185650-121188528, from -2000 bp to +879bp) was set as the "base", the numbers in the right panel represents the similarities to human. (B) The sequence alignments in these primates are adapted from Clustal Omega; the shaded characters represent the HREs predicted by the software as mentioned in Methods and the symbols in blue are the core hypoxia binding sites (HBS,

A/GCGTG). The green frame represents the location of the conserved binding site for CREB, which is one of the TFs involved in the transcription of hypoxia-responsive genes (13,17). **(C and D)** HIF-1 α protein expression in HeLa cells after hypoxia treatment. “20% O₂” represents the normal oxygen content, 1% O₂ is the oxygen content of the hypoxia-treated samples. The plots in **(D)** display the mean \pm SD of three independent experiments, *** $p < 0.001$ versus the 20% O₂ group. **(E and F)** DLR assays performed with the constructed plasmids containing different numbers of the predicted HREs in the human *FTMT* promoter region. The schematics on the left panels illustrate the HREs and their locations in the various constructs, while the right panels show the relative luciferase expression after 1% or 20% O₂ treatment. The value of the empty vector-treated cells (mock transfection, 20% O₂) is set to one. The plots display the mean \pm SD of three independent experiments. The numbers annotated in right panels of **(E)** and **(F)** on the plots of the treated group (1% O₂) represent the fold change vs each control group (20% O₂). Unedited blots of Figure 3C is shown in Supplementary Western Blots (SW2). To see this illustration in color, the reader is referred to the online version of this article at www.liebertpub.com/ars

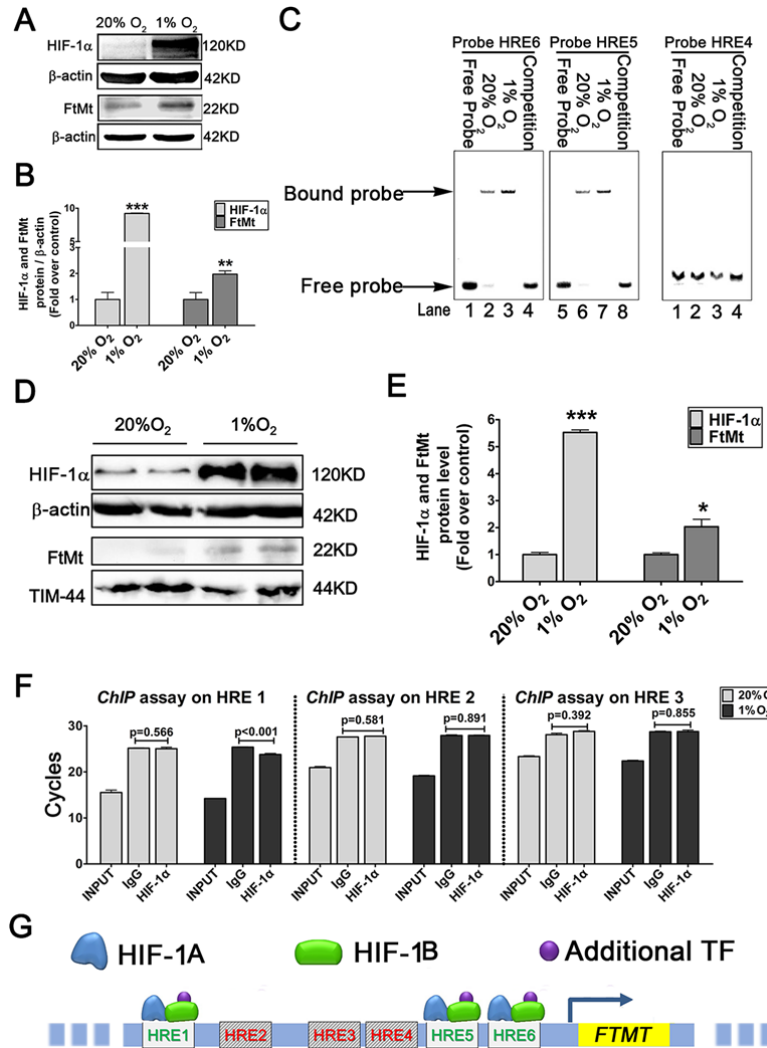


Figure 4 HIF-1α binds to putative HRE sites and activates FtMt expression

(A) HIF-1α and FtMt protein levels after exposure of U251 cells to 1% O₂ for 12 h. (B) Quantification of immunoblotting results. The plots display the mean ±SD of three independent experiments, ***p* < 0.01, ****p* < 0.001 versus the 20% O₂ group. (C) EMSA was carried out using hypoxia-treated U251 nuclear extract and biotin-labeled oligonucleotides containing HBS to detect the binding of HREs 4-6. Free Probe, no nuclear extract; Competition, a 200-fold excess of unlabeled probe was added. (D) The detection of HIF-1α and FtMt proteins after K562 cells were exposed to 1% O₂ for 14 h. For FtMt detection in K562 cells, mitochondrial fractions were used; TIM-44 was used as a loading control in each lane. (E) Quantification of the immunoblotting results. The plots display the mean ±SD of three independent experiments, **p* < 0.05, ****p* < 0.001 versus the 20% O₂

group. **(F)** Chromatin immunoprecipitation (ChIP) with K562 cell lysates using HIF-1 α antibodies. The amount of co-precipitated target DNA was evaluated by qRT-PCR using oligonucleotides specific for the regions containing the hypoxia response elements (HREs) as predicted *in silico*. **(G)** Scheme showing the positions of the HREs with detectable (green) and undetectable (red) HIF-1 α binding activities, as determined by the luciferase assay. Unedited blots of Figure 4 A and D are shown in Supplementary Western Blots (SW2). To see this illustration in color, the reader is referred to the online version of this article at www.liebertpub.com/ars

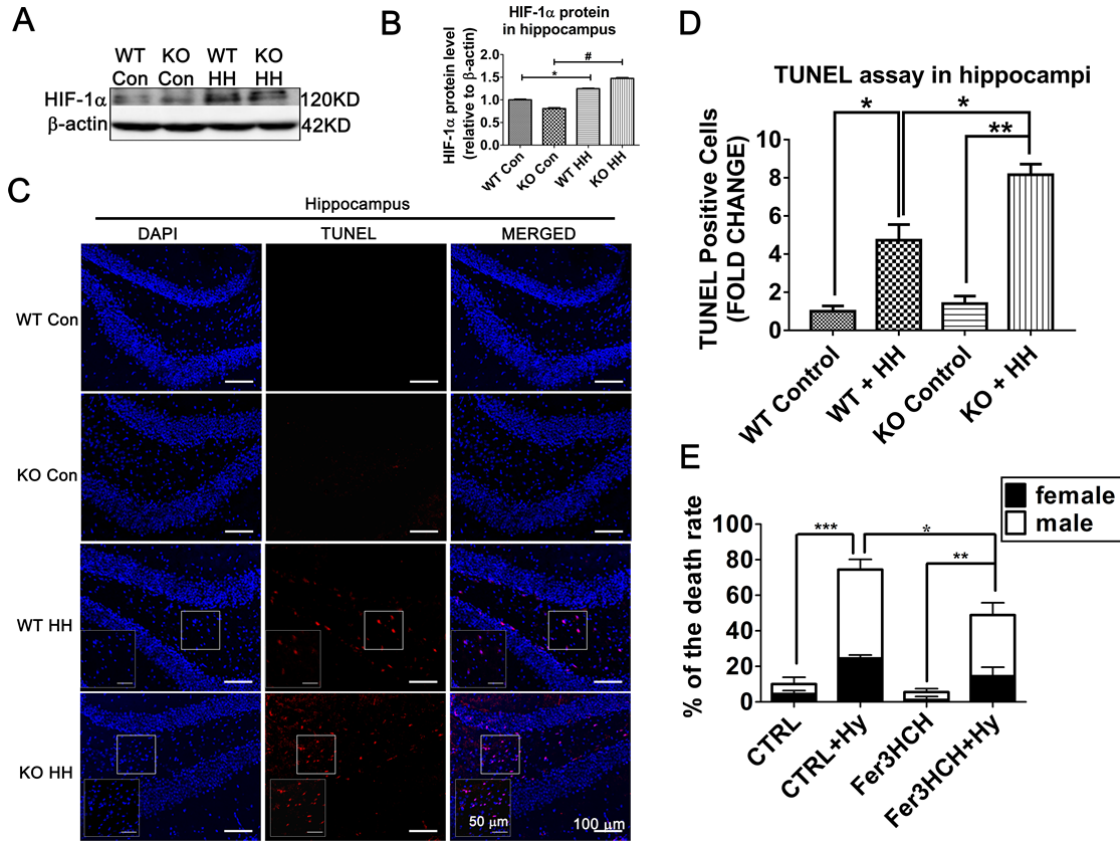


Figure 5 FtMt protects brain cells exposed to hypoxia *in vivo*

(A) HIF-1 α protein levels in mice hippocampi after 18 h continuous hypobaric hypoxia treatment as determined by immunoblotting (A) and (B) respective quantification. Error bars represent \pm SD, $n=4$, $*p < 0.05$ versus the WT control group, $\#p < 0.05$ versus the KO control group. (C) Cell death in mouse hippocampi was detected by DAPI and TUNEL staining as described in the Methods section. (D) DAPI-stained, TUNEL positive cells were counted using image J in three separate fields and are expressed as fold change normalized to the “WT Con” group. Values are presented as the mean \pm SD from four mice. (E) The death rates of *Drosophila* are shown as the mean \pm SD of three independent treatments, $n=90$. $*p < 0.05$, $**p < 0.01$, $***p < 0.001$ versus the groups indicated showed in the plots in (D) and (E). Unedited blots of Figure 5A is shown in Supplementary Western Blots (SW2). To see this illustration in color, the reader is referred to the online version of this article at www.liebertpub.com/ars

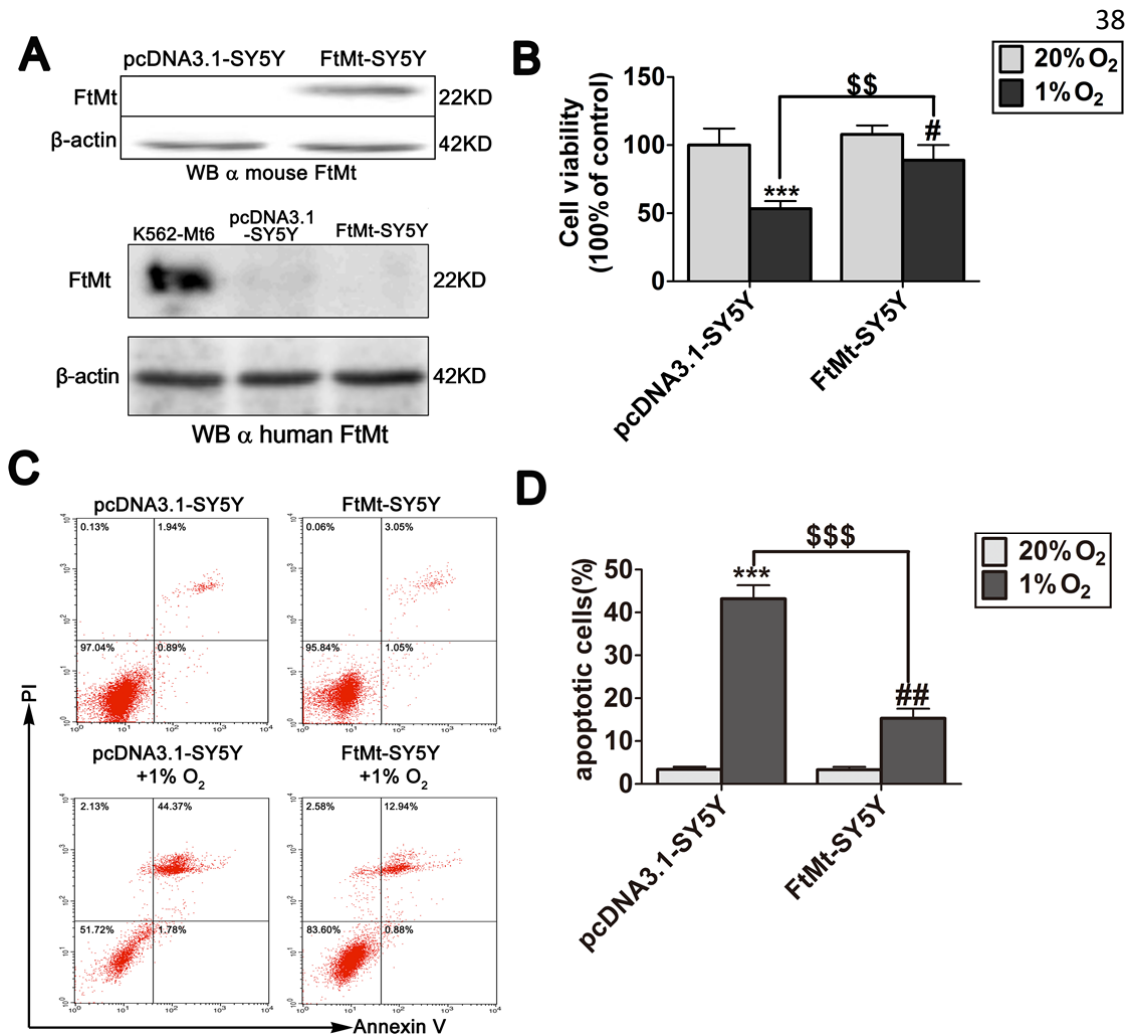


Figure 6 Overexpression of FtMt in SH-SY5Y cells attenuates hypoxia-induced brain cell death *in vitro*

(A) Immunoblot showing the exogenous (upper panel) and the endogenous (lower panel) FtMt levels in pcDNA3.1-SY5Y and FtMt-SY5Y cells. (B) Cell viability was measured by MTT assay in cells treated with or without 1% O₂ treatment for 24 h. Data were presented as mean percentages of the cell viability compared with untreated control cells \pm SD of three independent experiments. (C) pcDNA3.1-SY5Y and FtMt-SY5Y cells were exposed to 1% O₂ for 24 h and cell damage was measured by flow cytometry. The numbers in each panel in (C) represent the percentage of cells in each quadrant. (D) Quantification (summary of the number of Annexin V⁺/PI⁺ which indicates late apoptotic and necrotic cells and the number of Annexin V⁺/PI⁻ which represents early apoptotic cells) of the data from panel C, presented as the mean \pm SD of three independent experiments. *** p < 0.001 compared to

the untreated control cells; # $p < 0.05$, ## $p < 0.01$ versus the untreated FtMt-SY5Y cells; \$\$ $p < 0.01$, \$\$\$ $p < 0.001$ versus the indicated groups. Unedited blots of Figure 6A is shown in Supplementary Western Blots (SW2). To see this illustration in color, the reader is referred to the online version of this article at www.liebertpub.com/ars

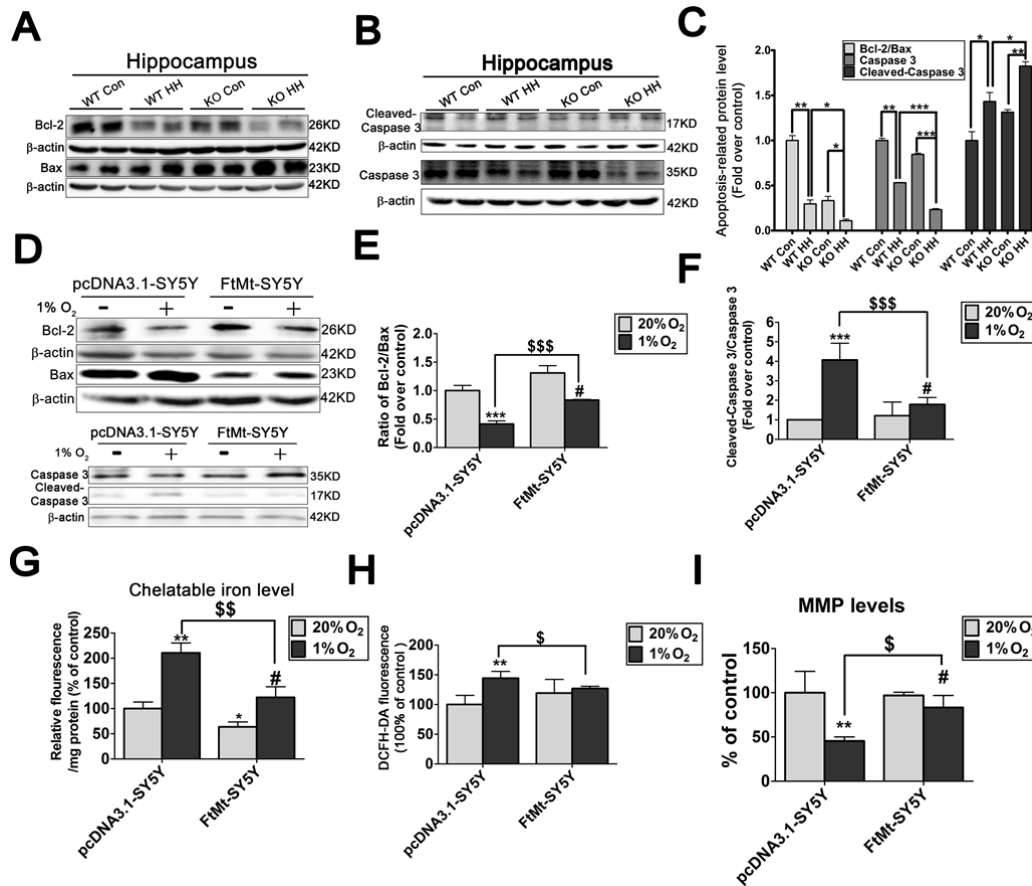


Figure 7 FtMt protects cells from hypoxia-induced activation of apoptosis-related proteins and oxidative damage

(A) The levels of Bcl-2 and Bax in the hippocampus of hypobaric hypoxia treated mice. (B) Cleaved-Caspase 3 and Caspase 3 in the mice hippocampi after HH treatment for 18 h. (C) Quantification of the bands in A and B. The plots are displayed as the mean \pm SD, $n=6$, $*p < 0.05$, $**p < 0.01$, $***p < 0.001$ versus the indicated groups. (D) The levels of Bcl-2, Bax, Cleaved-Caspase 3 and Caspase 3 in SH-SY5Y cells overexpressing FtMt after 1% O₂ hypoxia treatment for 24 h. (E and F) Quantification of the bands in D, displaying the mean \pm SD of three independent experiments. (G, H, I) Chelatable iron, ROS levels and mitochondria membrane potential (MMP) were measured with or without HH. All the data in (E), (F), (G), (H) and (I) are expressed as the mean \pm SD of three independent experiments. $*p < 0.05$, $**p < 0.01$, $***p < 0.001$ compared with the untreated control cells; $\#p < 0.05$, $###p < 0.01$ versus the untreated FtMt-SY5Y cells; $\$p < 0.05$, $$$p < 0.01$, $$$$p < 0.001$ versus the indicated group. Unedited blots of Figure 7A, B and D are shown in Supplementary Western Blots (SW3).

Supplemental Figure Legends

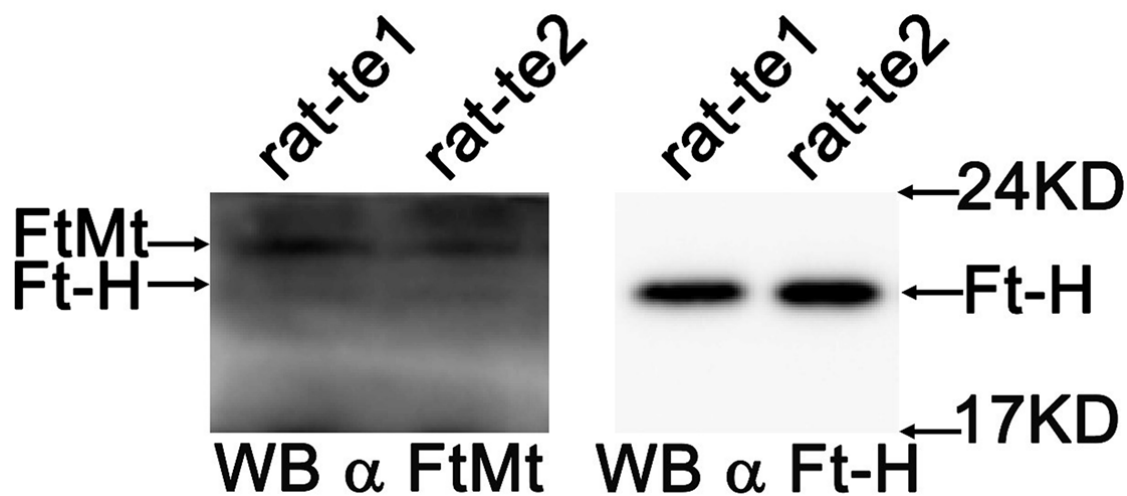


Figure S1. Specificity of FtMt antibody.

To test the specificity of the FtMt antibody in immunoblotting experiments, we performed experiments with rat testis lysates, which showing that the antibody has a much greater affinity to FtMt (22 KD) than ferritin-H (Ft-H) (21 KD). Rat testis total proteins lysates were resolved by SDS-PAGE and the FtMt and Ft-H protein levels were then detected by immunoblotting with the indicated antibodies. Unedited blots of Figure S1 is shown in Supplementary Western Blots (SW4).

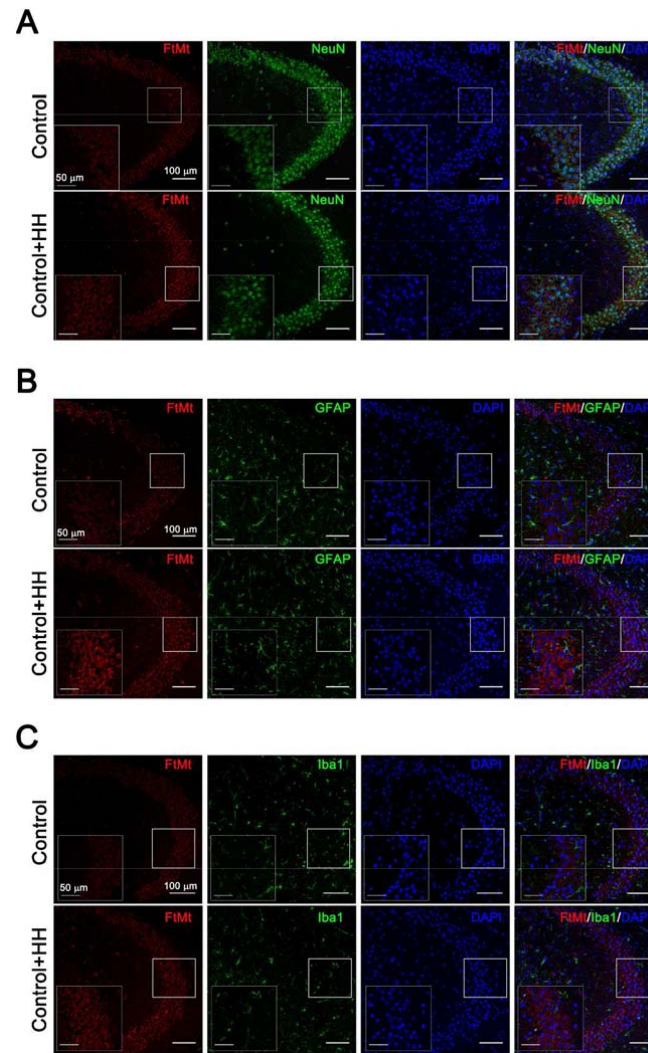


Figure S2. FtMt protein cellular distribution in the mouse hippocampus.

In order to study the cell-type expression pattern of FtMt in the mouse brain, we performed double immunofluorescence staining (double-IF) with antibodies specific for brain cell markers (green): NeuN for neurons (**A**), glial fibrillary acidic protein (GFAP) for astrocytes (**B**) and Iba1 for microglia (**C**) together with anti-FtMt (red) in the hippocampus region of HIF-1 α conditional knockout mice after HH treatment (Control group and Control + HH group).

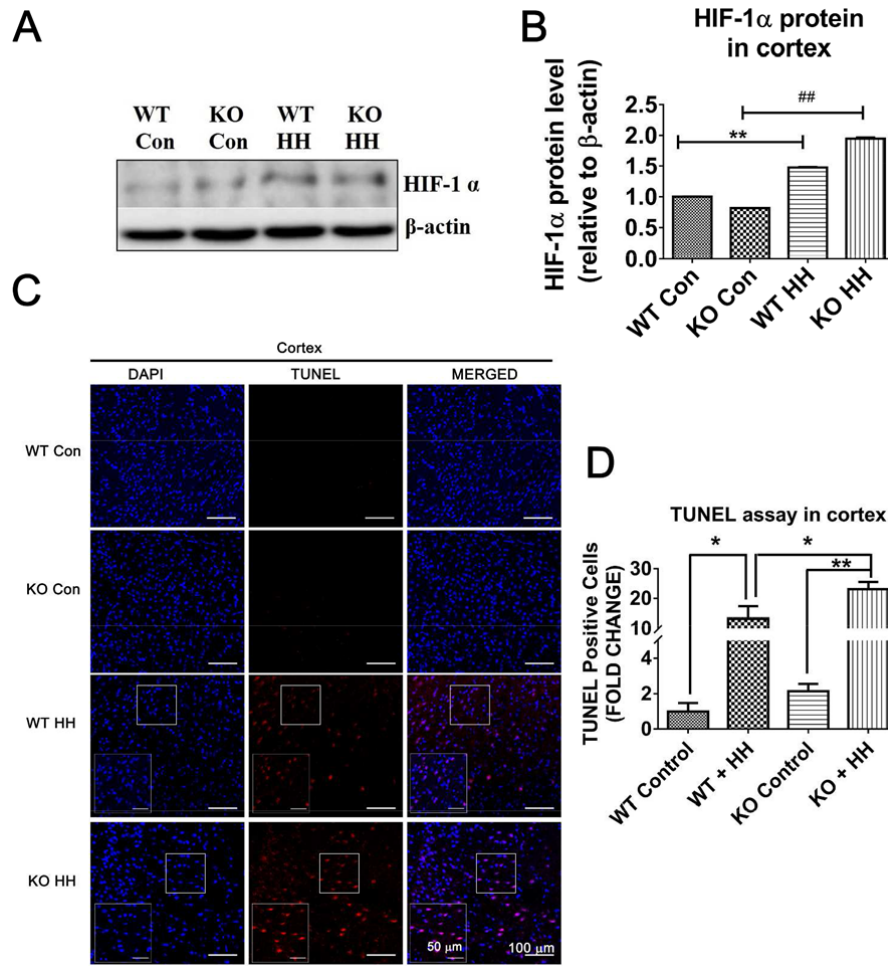


Figure S3. The detection of cell death in the mouse cortex after continuous HH treatment.

After 18 h continuous HH treatment, the HIF-1 α protein in the mouse cortices (A and B) was detected by immunoblotting. The plots represent the mean \pm SD, $n = 4$. $*p < 0.05$ versus the WT control group; $\#p < 0.05$ versus the KO control group. Cell death in mouse cortices was detected by DAPI and TUNEL staining, as described in the Methods section (C). DAPI-stained, TUNEL positive cells were counted in three separate fields, using image J, and are presented as fold change normalized to the “WT Con” group (D). Values are presented as the mean \pm SD from four mice. $*p < 0.05$, $**p < 0.01$ versus the groups indicated in the plots. Unedited blots of Figure S3 A is shown in Supplementary Western Blots (SW4).

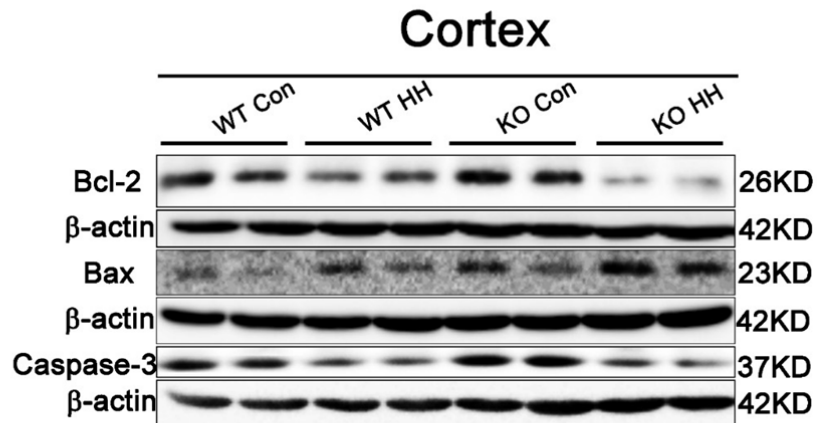
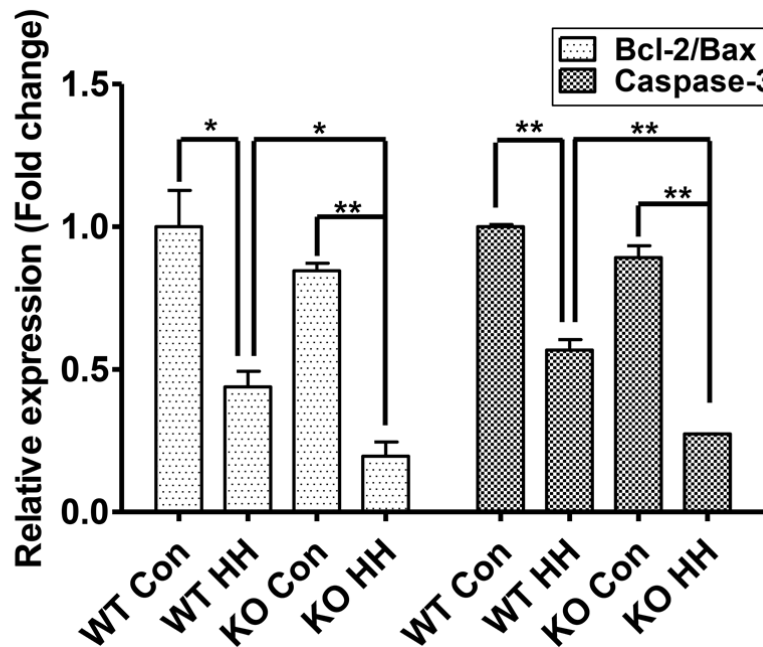
A**B**

Figure S4. The detection of apoptosis-related proteins in the mouse cortex after HH treatment.

To further investigate the apoptotic pathway induced by hypoxia, *Ftmt*^{-/-} mice were placed into the hypoxic chamber for 18 h hypobaric hypoxia, after which apoptosis-related proteins were assessed. (A) The ratio of Bcl-2/Bax and the Caspase-3 levels in the cortex of hypobaric hypoxia treated mice. (B) Quantification of the bands in panel A. The plots are displayed as the mean \pm SD, $n=6$, * $p < 0.05$, ** $p < 0.01$ versus the indicated groups.

Unedited blots of Figure S4 A is shown in Supplementary Western Blots (SW4).

